Acta Geochim (2016) 35(4):421–427
DOI 10.1007/s11631-016-0105-7

ORIGINAL ARTICLE

Standard-sample bracketing calibration method combined with Mg as an internal standard for silicon isotopic compositions using multi-collector inductively coupled plasma mass spectrometry

Honglin Yuan[1] · Cheng Cheng[1] · Kaiyun Chen[1] · Zhian Bao[1]

Received: 12 January 2016 / Revised: 12 March 2016 / Accepted: 28 March 2016 / Published online: 16 April 2016

Abstract Silicon isotope analysis traditionally uses a standard-sample bracketing (SSB) method that relies upon greater instrument stability than can be consistently expected. The following proposed method reduces the level of instrumental stability required for the analysis process and provides a valid solution for high-precision and accurate studies of Si isotopic compositions. Rock samples were dissolved by using alkali fusion and acidification. Silicon isotopes were purified with an ion exchange resin. Interfering peaks for isotopes were separated by using a Nu Plasma 1700 multi-collector inductively coupled plasma mass spectrometry (MS) system in high-resolution mode ($M/\Delta M > 8000$ RP). Two magnesium isotopes (^{25}Mg and ^{26}Mg) and three silicon isotopes (^{28}Si, ^{29}Si, and ^{30}Si) were analyzed in the same data collection cycle. Mg isotopes were used as an internal standard to calibrate the mass discrimination effects in MS analysis of Si isotopes in combination with the SSB method in order to reduce the effects of MS interference and instrumental mass discrimination on the accuracy of measurements. The conventional SSB method without the Mg internal standard and the proposed SSB method with Mg calibration delivered consistent results within two standard deviations. When Mg was used as an internal standard for calibration, the analysis precision was better than 0.05 ‰ amu.

Keywords Si isotope · Mg internal standard · MC-ICP-MS · Rock samples · High resolution

✉ Honglin Yuan
sklcd@nwu.edu.cn

[1] State Key Laboratory of Continental Dynamics, Department of Geology, Northwest University, Collaborative Innovation Center of Continental Tectonics, Xi'an 710069, China

1 Introduction

Silicon is the second-most abundant element in Earth's crust; it makes up the skeleton of rocks and has stable chemical properties. Silicon has three stable isotopes: ^{28}Si, ^{29}Si, and ^{30}Si with relative abundances of 92.23 %, 4.67 %, and 3.1 % respectively (Cardinal et al. 2003; Georg et al. 2007). Researchers have conducted numerous studies on Si isotopes to better understand magmatism, meteorites, hydrothermal mineral deposits, clay minerals, the ocean silicon cycle, biological silicate, and fractionation of silicate melts and metallic melts (Brzezinski et al. 2003; Armytage et al. 2011; Opfergelt et al. 2011; Armytage et al. 2012; Opfergelt et al. 2013; Savage et al. 2013; Hin et al. 2014; Zhu et al. 2014). Studies on silicon isotopes have not only revealed Earth's evolutionary history (Georg et al. 2007; Armytage et al. 2011; Ziegler et al. 2010; Savage and Moynier 2013; Savage et al. 2013) but also are very important in explaining ore genesis (as it pertains to mineral resources) and in research on the climate and carbon cycle (Dugdale et al. 2004; Pringle et al. 2013; Hou et al. 2014).

Si isotopic composition is normally determined by using multi-collector inductively coupled plasma mass spectrometry (MC-ICP-MS), whose accuracy and precision are mainly affected by interfering mass spectrometry (MS) peaks for isobaric heterotopes, instrumental mass discrimination effects, and the stability of the sample injection system. Standard-sample bracketing (SSB) is normally used to calculate Si isotopic composition. To calibrate the instrumental mass discrimination, the SSB method requires identical instrumental conditions and excellent stability during analysis of the standard and actual samples. In practice, each sample needs to be measured more than three times, and the mean value of the measurements is

calculated as the Si isotopic composition of the sample to obtain stable and reliable results. Fluctuations in instrumental conditions that affect the accuracy of the isotopic ratio analyses are mainly caused by changes in the sensitivity of the sample injection system or in the mass discrimination effects in the MS system. These are usually calibrated using two isotopes of elements with similar atomic weights (e.g., adding ^{203}Tl and ^{205}Tl for isotopic analysis of Pb). Because of their similar relative atomic masses to those of Si isotopes, the Mg isotopes ^{25}Mg and ^{26}Mg can be used to calibrate mass discrimination effects. Cardinal et al. (2003), Zambardi and Poitrasson (2011) added magnesium into silicon samples and standard solutions to calibrate the changes in the Si isotopic composition caused by changes in the mass discrimination effects from variations in the space charge effect or sample injection conditions. However, because of previously experienced hardware limitations, they analyzed Mg and Si isotopes in two different data collection cycles during the measurement process; simultaneous analysis of Mg and Si isotopes could not be achieved, and so the changes in the measured Si isotopic composition caused by variations in the instrumental conditions were not effectively calibrated.

In this study, interfering peaks were separated by using the high-resolution mode of the large dimension MC-ICP-MS system (Nu Plasma 1700). Mg was used as the internal standard, and the physical positions of the detectors at the high- and low-mass sides of the instrument were moved to the extremes to slightly extend the mass dispersion limit of the MC-ICP-MS system, allowing for the analysis of Mg (^{25}Mg and ^{26}Mg) and Si isotopes in the same data collection cycle, thus achieving simultaneous collection of Mg isotope and Si isotope signals. The Mg isotopes were used to calibrate the fractionation effect during the Si isotopic analysis to obtain accurate Si isotopic compositions.

2 Methods

2.1 Reagents

The experiments used AR-grade nitric acid and hydrochloric acid that were distilled twice with a PFA Savillex DST-1000 sub-boiling still (Minnetonka, USA). Ultrapure water was purified with Milli-Q Element (Elix-Millipore, USA) (18.2 MΩ/cm). The standard solutions were Alfa Si and Alfa Mg (Si: stock no. 38717; Mg: stock no. 14430, 2 % HNO_3, plasma standard solution, Specpure, Alfa Aesar, Johnson Matthey Company). NaOH (LOT: 10165572, Alfa Aesar, Johnson Matthey Company) was used as the fluxing agent for the fusion test. A Bio-Rad polypropylene ion exchange column was used for the purification test with a Bio-Rad AG50-X12 cation exchange resin (Catalog # 142-1651, Bio-Rad Laboratories Inc., CA, USA).

2.2 Sample dissolution

Rock samples were fused by using NaOH as the fluxing agent and dissolved with HCl according to the method presented in a previous study (Georg et al. 2006). To avoid contamination during sample fusion in the Muffle furnace, 5 and 30 mL silver crucibles fabricated in the laboratory (Fig. 1) were used as melting vessels in this study. The samples and crucibles in contact with the samples were kept inside a relatively clean and large crucible during the entire sample fusion process. The weighing of the sample, addition of the fluxing agent, and transfer of the small crucibles into the large crucible were performed with a class 100 clean bench to reduce the background level during the test process. The specific sample dissolution procedure was as follows: within the clean bench, 10 mg of powdery sample was evenly mixed with 200 mg powdery NaOH and placed into a 5 mL silver crucible. This crucible was then covered and transferred into a 30 mL crucible with a lid. The large crucible was placed into a Muffle furnace, where the sample was fused at 730 °C for 10 min. Upon cooling, the 5 mL small silver crucible containing the melt was placed into a Teflon vial (30 mL, Savillex Corporation, Minnesota, USA), and 20 mL ultrapure water was added. The mixture was ultrasonicated for 15 min, allowed to settle for 24 h, and ultrasonicated for another 15 min. The solution inside the Teflon vial was diluted and acidified to pH 2.2 with hydrochloric acid (Fitoussi et al. 2009) and then heated at 40 °C for 15 min to accelerate the dissolution of hydroxide.

2.3 Chemical separation

Si isotopes were purified by using 2 mL cation exchange resin (AG 50-X12). Because the active ion of the resin was

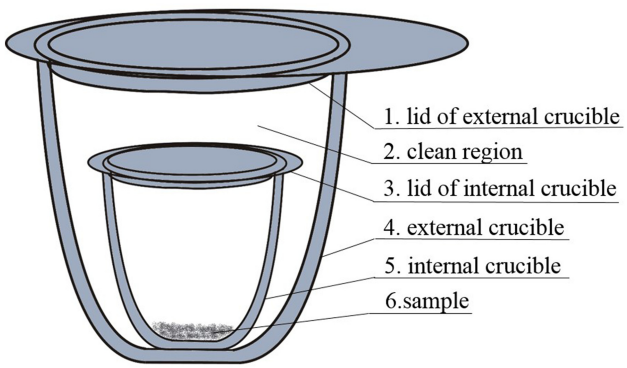

Fig. 1 NaOH fusion in silver crucible

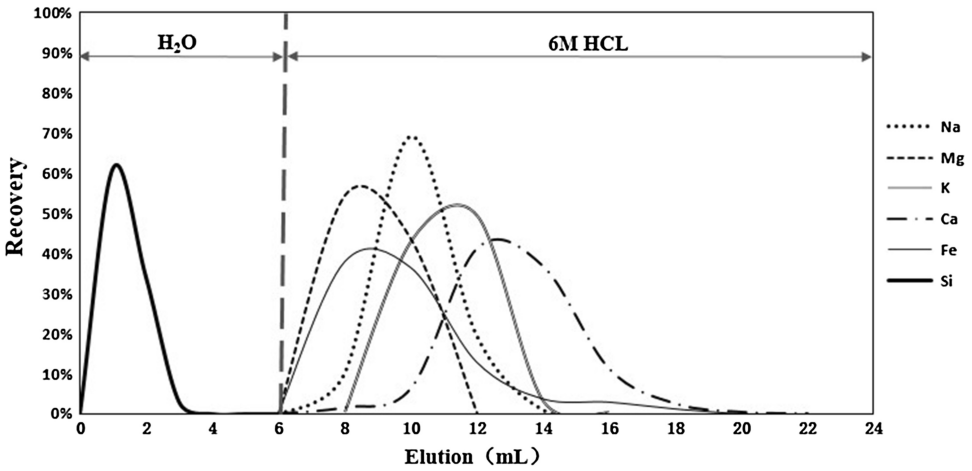

Fig. 2 Elution curve of Si in rock sample solution

H^+, the resin did not adsorb anions but effectively adsorbed cations. Si was present in the solution in the form of $H_3SiO_4^-$ (Georg et al. 2006). Si could be directly eluted with the ultrapure water, and cations of substrate elements such as Na^+, K^+, Mg^{2+}, Al^{3+} etc. were adsorbed onto the resin; thus, Si was separated from the cations (Fig. 2). The recovery rate of Si isotopes was greater than 98 %, and the background level during the entire process was less than 20 ng. Table 1 presents the separation procedure.

2.4 Apparatus and data processing

Instrumental analysis was performed with a high-resolution Nu Plasma 1700 MC-ICP-MS system (Nu Instruments, UK) installed in the State Key Laboratory of Continental Dynamics, Northwest University, Xi'an, China. The Nu Plasma 1700 system was equipped with three ion-counting multipliers and 16 Faraday cups. The high- and low-mass sides each had three independently movable Faraday cups and two independently movable slits before each Faraday cup to achieve separate resolution of the interfering peaks on the high- and low-mass sides (Fig. 3). The highest $RP_{(edge\ 5,\ 95\%)}$ of the MS system was greater than 20,000. In this study, the outermost Faraday cups H8 and L7 were moved to the extreme positions, and the slits before the Faraday cup were moved to the two sides to receive ^{30}Si and ^{25}Mg signals simultaneously. Table 2 presents the detectors for the other isotopes. In this study, the resolution was in the range of 8000–10,000 RP, and data were collected in static mode. The ratios of Si/Mg in the solution were about 1 and the sensitivity of Si was about 2 V/ppm. During the Si isotope test, the background noise (<50 mV) was deducted as the on-peak zero (OPZ). Samples were injected in the wet state (Zambardi and Poitrasson 2011). Table 2 presents the instrument parameters.

For data calibration purposes, the fractionation factor was calculated from the measured ratio between a pair of DSM3 Mg standard isotopes (^{25}Mg–^{26}Mg) and the reference isotopic ratio by using the power index method. The Si isotopic ratios $^{29}Si/^{28}Si$ and $^{30}Si/^{28}Si$ were calibrated through fractionation. The Si isotopic compositions of the samples $\{\delta^{29}Si = [(^{29}Si/^{28}Si)_{sample}/(^{29}Si/^{28}Si)_{standard} - 1] \times 1000;\ \delta^{30}Si = [(^{30}Si/^{28}Si)_{sample}/(^{30}Si/^{28}Si)_{standard} - 1] \times 1000\}$ were calculated by using the SSB method. The

Table 1 Separation scheme of silicon isotopes

Step	Eluent	Volume	Function
1	3 mol/L HCL	5 mL	Pre-washing
2	6 mol/L HCL	5 mL	Pre-washing
5	3 mol/L HCL	5 mL	Pre-washing
7	H_2O	>10 mL until pH = 7	Resin equilibration
8	Sample addition	1 mL (~28 μg Si)	Sample loading
9	H_2O	2 mL × 3	Si collection
If the resin was used only once, the procedure was completed; otherwise, the resin was rinsed for future use according to the following procedure			
10	6 mol/L HCL	5 mL × 3	Resin rinsing
11	6 mol/L HNO_3	5 mL	Resin rinsing
12	3 mol/L HCL	5 mL	Resin rinsing

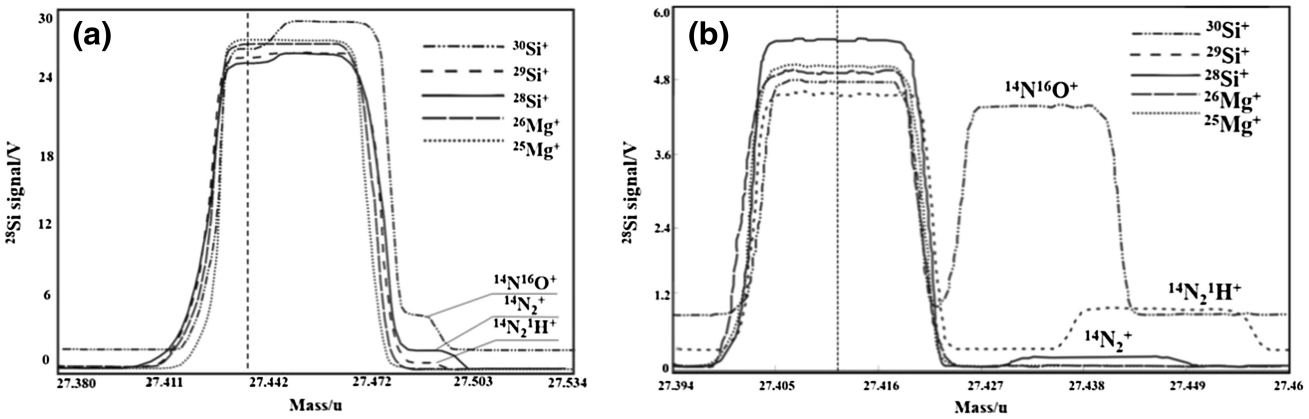

Fig. 3 Mass scan of Si isotopes and polyatomic interference with MC-ICP-MS: mass spectrum peaks at **a** low resolution (1000 RP) and **b** high resolution (8000 RP)

Table 2 Operating conditions for Si isotope determination using Nu Plasma 1700 MC-ICP-MS

MS conditions	Instrument parameters
RF power	1300 W
Cooling gas flow rate	13.0 L/min
Auxiliary gas flow rate	1.0 L/min
Nebulizer gas flow rate	0.85 L/min
Accelerating voltage	6000 V
Uptake rate	100 μL/min
Spray chamber	*Double-pass cyclonic spray chamber* (ESI, USA)
Cones	Ni (1.15 mm sampler cone + 0.6 mm skimmer cone)
Torch	Quartz external tube, sapphire central tube
Resolution (edge: 5.95 %)	8000–10,000 RP
Faraday cup	H8 (^{30}Si), H6 (^{29}Si), H3 (^{28}Si), L5 (^{25}Mg), L7 (^{26}Mg)

Alfa Si standard solution was calibrated according to NIST NBS 28 and used as the Si isotope reference standard.

2.5 Internal standard-based calibration

The abundances of ^{26}Mg and ^{25}Mg are 11.01 % and 10.00 %, respectively. They can be used to effectively calculate the mass discrimination effect in MS during Si isotope measurement (Zambardi and Poitrasson 2011). Although $^{24}MgH^+$ interferes with $^{25}Mg^+$, the influence of this hydride on $^{26}Mg/^{25}Mg$ is less than 0.02 ‰ (Engström et al. 2006). The difference in mass between ^{25}Mg and ^{30}Si is 20 %, which is greater than the specified mass dispersion (17 %) for MC-ICP-MS. Therefore, previous researchers have analyzed Mg and Si in two different cycles (Cardinal et al. 2003), but the fluctuations in instrumental conditions resulted in different Si isotopic compositions of the samples due to the fractionation effect of Mg and Si isotopes being determined in different cycles, which affected the accuracy of the Si isotopic compositions. In this study, the outermost Faraday cups H8 and L7 on the high- and low-mass sides were manually moved to the extreme edges, and the ion lenses were adjusted to appropriately compress the mass peaks with the zoom lens to put the Mg isotopes ($^{25}Mg^+$, $^{26}Mg^+$) and Si isotopes ($^{28}Si^+$, $^{29}Si^+$ and $^{30}Si^+$) into the same cycle without changing the magnetic field during the test. This increased the analysis efficiency and data quality.

According to the conventional power index calibration method, the fractionation factor f_{Mg} of Mg isotopes in MS analysis can be obtained from standard samples with known isotopic ratios:

$$f_{Mg} = \ln\left(\frac{\left(^{26}Mg/^{25}Mg\right)_{ture}}{\left(^{26}Mg/^{25}Mg\right)_{measure}}\right) \Big/ \ln\left(\frac{\left(Mass^{26}Mg\right)}{\left(Mass^{25}Mg\right)}\right) \quad (1)$$

$$f_{Si} = \ln\left(\frac{\left(^{29}Si/^{28}Si\right)_{ture}}{\left(^{29}Si/^{28}Si\right)_{measure}}\right) \Big/ \ln\left(\frac{(Mass^{29}Si)}{(Mass^{28}Si)}\right) \quad (2)$$

If there is a simple linear relationship between the fractionation factors of Mg and Si, then

$$f_{Si} = a \times f_{Mg}. \quad (3)$$

Based on f_{Mg}, the Si isotopic ratio in the sample can be calculated as follows:

$$\left(\frac{^{29}Si}{^{28}Si}\right)_{ture} = \left(\frac{^{29}Si}{^{28}Si}\right)_{measure} \times \left(\frac{Mass^{29}Si}{Mass^{28}Si}\right)^{a\times f_{Mg}}. \quad (4)$$

The correlation between $\ln(^{29}Si/^{28}Si)_{measure}$ and $\ln(^{26}Mg/^{25}Mg)_{measure}$ can be determined as follows:

$$\ln\left(\frac{^{29}Si}{^{28}Si}\right)_{measure} = 0.897 \times a \times \ln\left(\frac{^{26}Mg}{^{25}Mg}\right)_{measure} + \left(\ln\left(\frac{^{29}Si}{^{28}Si}\right)_{ture} - 0.897 \times a \times \left(\frac{^{26}Mg}{^{25}Mg}\right)_{ture}\right), \quad (5)$$

where a is calculated from the slope S of the plot of $\ln(^{29}Si/^{28}Si)_{measure}$ versus $\ln(^{26}Mg/^{25}Mg)_{measure}$:

$$S = 0.897 \times a \quad (6)$$

The isotopic ratios of Si and Mg measured in the same analysis cycle in a mixed solution are plotted in Fig. 4. The slope of the plot is 0.882, and a was calculated to be 0.9833. Within the same analysis cycle, inserting a into Eq. 3 obtained the fractionation factor of Si. Inserting a into Eq. 4 obtained the Si isotopic composition of the samples. Differences in instrumental conditions, especially due to instrumental repair such as the replacement of a cone or torch, usually cause considerable changes in the absolute values of Si and Mg isotopic ratios; the variation in S can reach 25 % (Cardinal et al. 2003). Therefore, calculations should only be based on $\ln(^{29}Si/^{28}Si)_{measure}$ and $\ln(^{26}Mg/^{25}Mg)_{measure}$ with data obtained within the same analysis section under identical instrumental analysis conditions.

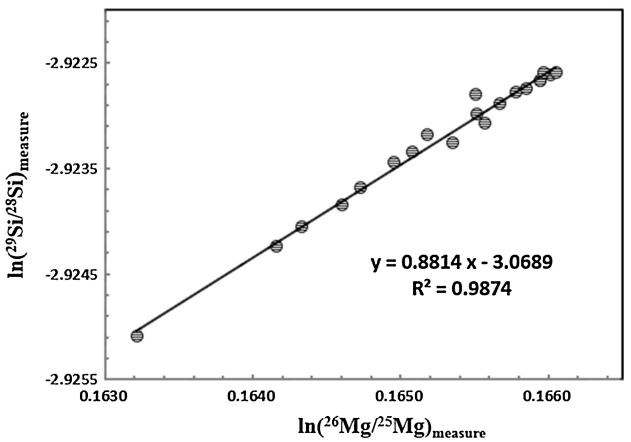

Fig. 4 MC-ICP-MS measured ratios of ln $^{29}Si/^{28}Si$ versus ln $^{26}Mg/^{25}Mg$

3 Mass spectrometry resolution and results

3.1 Resolution and interfering peaks in mass spectrometry spectra

The MC-ICP-MS analysis of the three silicon isotopes was subjected to the following interferences: ($^{14}N_2^+$, $^{12}C^{16}O^+$) for $^{28}Si^+$, ($^{14}N_2^1H^+$, $^{12}C^1H^{16}O^+$, $^{15}N^{14}N^+$) for $^{29}Si^+$, and $^{30}Si^+$($^{14}N^{16}O^+$) for $^{30}Si^+$. These interfering peaks cannot be effectively separated in conventional low-resolution mode (<1000 RP) and are at the high-mass side of the Si isotopes. Thus, a magnetic field deviating from the peak center is normally used for measurements on a narrow platform without interference (Fig. 3a) (Zhang et al. 2014). However, slight disturbances in the testing conditions result in a shift of mass spectral peaks, which can affect the accuracy of the analysis results. In this study, the resolution of the MS system was increased to above 8000 RP, and the ion lens, focusing lens, and collector slits were adjusted. This resulted in complete separation of the mass spectral peaks for $^{28}Si^+$, $^{29}Si^+$, $^{30}Si^+$, $^{25}Mg^+$, and $^{26}Mg^+$ with good peak shapes from interfering peaks (Fig. 3b), thus ensuring the reliability of the Si isotopic analysis results.

3.2 Measurement results

NBS-28 and IRMM-018a are commonly used international reference standards in Si isotope studies (Reynolds et al. 2007). In addition, the Si isotopic composition of the BHVO-2 standard rock sample has been reported (Zambardi and Poitrasson 2011). In this study, the Mg internal standard plus SSB calibration method and the SSB calibration method without an internal standard were used to determine the Si isotopic compositions of IRMM-018a and BHVO-2, respectively (Table 3).

The results indicate that the Mg isotopic compositions obtained by SSB calibration plus the Mg internal standard and by SSB calibration without the internal standard were consistent within the error range and agreed with the reported values. This indicates that both methods delivered an accurate Si isotopic composition. Overall, the Mg internal standard plus SSB method resulted in more stable relative errors than the SSB method without an

Table 3 Si isotopic compositions of standard references BHVO-2 and IRMM18a

Sample	Si isotopic composition (‰), this study		Reported Si isotopic value (‰)		
	$\delta^{29}Si$	$\delta^{30}Si$	$\delta^{29}Si$	$\delta^{30}Si$	References
BHVO-2	-0.14 ± 0.06[a]	-0.28 ± 0.08[a]	-0.15 ± 0.06	-0.28 ± 0.09	Savage and Moynier (2013)
	($n = 9$)	($n = 9$)	-0.14 ± 0.09	-0.29 ± 0.10	Savage et al. (2013)
			-0.15 ± 0.09	-0.28 ± 0.12	Pringle et al. (2013)
	-0.13 ± 0.08[b]	-0.27 ± 0.08[b]	-0.15 ± 0.08	-0.28 ± 0.14	Armytage et al. (2012)
	($n = 8$)	($n = 8$)	-0.14 ± 0.08	-0.29 ± 0.09	Savage et al. (2011)
			-0.14 ± 0.05	-0.27 ± 0.08	Zambardi and Poitrasson (2011)
			-0.14 ± 0.05	-0.27 ± 0.10	Savage et al. (2010)
			-0.16 ± 0.15	-0.32 ± 0.15	Fitoussi et al. (2009)
IRMM-18a	-0.89 ± 0.08[a]	-1.83 ± 0.08[a]	-0.79 ± 0.03	-1.55 ± 0.25	Ziegler et al. (2010)
	($n = 7$)	($n = 7$)	-0.97 ± 0.40	-1.65 ± 0.67	Ziegler et al. (2010)
	-0.88 ± 0.08[b]	-1.82 ± 0.15[b]			
	($n = 11$)	($n = 11$)			

[a] Calibrated with internal standard + SSB method

[b] Calibrated with SSB method without internal standard. All errors are expressed as 2SD

internal standard. Thus, this new method reduces the level of instrumental stability required for the analysis process which is very important for applications involving the addition of spikes for Si.

4 Conclusion

In this study, rock samples were dissolved by alkali fusion and acidification, and silicon isotopes were purified with ion exchange resin for a recovery rate above 98 %. Interfering peaks for isotopes were separated by using the Nu Plasma 1700 MC-ICP-MS system in high-resolution mode. Magnesium and silicon isotopes were analyzed in the same test cycle. MS interference for silicon isotopes was completely isolated by using the Nu Plasma 1700 MC-ICP-MS system at a resolution of 8000 RP. The outermost Faraday cups were manually moved to the extreme edges of the instrument; this allowed the Mg and Si isotopes to be analyzed in the same cycle and established an Mg internal standard plus SSB calibration analysis method to obtain accurate Si isotopic compositions. Compared with the Si isotopic composition obtained by the SSB method without an internal standard, the proposed method features stable and reliable accuracy and precision. The Si isotopic composition obtained after calibration with the Mg internal standard was closer to the actual value, which is very important for applications involving the addition of a spikes for Si.

Acknowledgments This study was funded by the National Natural Science Foundation of China (Grant Nos. 41427804, 41421002, 41373004), Beijing SHRIMP Center Open Foundation, and Program for Changjiang Scholars and Innovative Research Team in University (Grant No. IRT1281) and the MOST Research Foundation from the State Key Laboratory of Continental Dynamics (BJ08132-1).

References

Armytage RMG, Georg RB, Savage PS, Williams HM, Halliday AN (2011) Silicon isotopes in meteorites and planetary core formation. Geochim Cosmochim Acta 75:3662–3676

Armytage RMG, Georg RB, Williams HM, Halliday AN (2012) Silicon isotopes in lunar rocks: implications for the Moon's formation and the early history of the Earth. Geochim Cosmochim Acta 77:504–514

Brzezinski MA, Jones JL, Bidle KD, Azam F (2003) The balance between silica production and silica dissolution in the sea: insights from Monterey Bay, California, applied to the global data set. Limnol Oceanogr 48:1846–1854

Cardinal D, Alleman LY, de Jong J, Ziegler K, André L (2003) Isotopic composition of silicon measured by multicollector plasma source mass spectrometry in dry plasma mode. J Anal At Spectrom 18:213–218

Dugdale RC, Lyle M, Wilkerson FP, Chai F, Barber RT, Peng TH (2004) Influence of equatorial diatom processes on Si deposition and atmospheric CO_2 cycles at glacial/interglacial timescales. Paleoceanography 19:143–168

Engström E, Rodushkin I, Baxter DC, Öhlander B (2006) Chromatographic purification for the determination of dissolved silicon isotopic compositions in natural waters by high-resolution multicollector inductively coupled plasma mass spectrometry. Anal Chem 78:250–257

Fitoussi C, Bourdon B, Kleine T, Oberli F, Reynolds BC (2009) Si isotope systematics of meteorites and terrestrial peridotites:

implications for Mg/Si fractionation in the solar nebula and for Si in the Earth's core. Earth Planet Sci Lett 287:77–85

Georg RB, Reynolds B, Frank M, Halliday A (2006) New sample preparation techniques for the determination of Si isotopic compositions using MC-ICPMS. Chem Geol 235:95–104

Georg RB, Halliday AN, Schauble EA, Bc R (2007) Silicon in the Earth's core. Nature 447:1102–1106

Hin RC, Fitoussi C, Schmidt MW, Bourdon B (2014) Experimental determination of the Si isotope fractionation factor between liquid metal and liquid silicate. Earth Planet Sci Lett 387:55–66

Hou K, Li Y, Gao J, Liu F, Qin Y (2014) Geochemistry and Si–O–Fe isotope constraints on the origin of banded iron formations of the Yuanjiacun Formation, Lvliang Group, Shanxi, China. Ore Geol Rev 57:288–298

Opfergelt S, Georg RB, Delvaux B, Cabidoche YM, Burton KW, Halliday AN (2011) Silicon isotopes and the tracing of desilication in volcanic soil weathering sequences, Guadeloupe. Chem Geol 326–327:113–122

Opfergelt S, Burton KW, Strandmann PAEPV, Gislason SR, Halliday AN (2013) Riverine silicon isotope variations in glaciated basaltic terrains: implications for the Si delivery to the ocean over glacial–interglacial intervals. Earth Planet Sci Lett 369–370:211–219

Pringle EA, Savage PS, Badro J, Barrat JA, Moynier F (2013) Redox state during core formation on asteroid 4-Vesta. Earth Planet Sci Lett 373:75–82

Reynolds BC, Aggarwal J, André L, Baxter D, Beucher C, Brzezinski MA, Engstrom E, Georg RB, Land M, Leng MJ (2007) An inter-laboratory comparison of Si isotope reference materials. J Anal At Spectrom 22:561–568

Savage PS, Moynier F (2013) Silicon isotopic variation in enstatite meteorites: clues to their origin and Earth-forming material. Earth Planet Sci Lett 361:487–496

Savage PS, Georg RB, Armytage RMG, Williams HM, Halliday AN (2010) Silicon isotope homogeneity in the mantle. Earth Planet Sci Lett 295:139–146

Savage PS, Georg RB, Williams HM, Burton KW, Halliday AN (2011) Silicon isotope fractionation during magmatic differentiation. Geochim Cosmochim Acta 75:6124–6139

Savage PS, Georg RB, Williams HM, Halliday AN (2013) Silicon isotopes in granulite xenoliths: insights into isotopic fractionation during igneous processes and the composition of the deep continental crust. Earth Planet Sci Lett 365:221–231

Zambardi T, Poitrasson F (2011) Precise determination of silicon isotopes in silicate rock reference materials by MC-ICP-MS. Geostand Geoanal Res 35:89–99

Zhang A, Zhang J, Zhang R, Xue Y (2014) Modified enrichment and purification protocol for dissolved silicon isotope determination in natural waters. J Anal At Spectrom 29:2414–2418

Zhu C, Liu Z, Schaefer A, Wang C, Zhang G, Gruber C, Ganor J, Georg RB (2014) Silicon isotopes as a new method of measuring silicate mineral reaction rates at ambient temperature. Procedia Earth Planet Sci 10:189–193

Ziegler K, Young ED, Schauble EA, Wasson JT (2010) Metal–silicate silicon isotope fractionation in enstatite meteorites and constraints on Earth's core formation. Earth Planet Sci Lett 295:487–496